# Electronic structure of one-dimensional cuprates

K. Maiti and D. D. Sarma*
*Solid State and Structural Chemistry Unit, Indian Institute of Science, Bangalore 560 012, India*

T. Mizokawa and A. Fujimori
*Department of Physics, University of Tokyo, Bunkyo-ku, Tokyo 113, Japan*
(Received 24 February 1997; revised manuscript received 8 August 1997)

We have investigated the electronic structures of one-dimensional antiferromagnetic insulators $Ca_2CuO_3$ and $Sr_2CuO_3$ combining electron spectroscopic measurements and various calculations. While calculations based on a local-spin-density approach for the real magnetic structures fail to yield an insulating state, from our experiments we estimate the intrinsic band gaps in these materials to be about 1.7 eV ($Ca_2CuO_3$) and 1.5 eV ($Sr_2CuO_3$). Analysis of the core-level and the valence-band spectra in terms of model many-body Hamiltonians show that the charge-transfer energy $\Delta$ for these one-dimensional systems is significantly smaller than other cuprates, such as the high-$T_c$ oxides (two-dimensional) and CuO (three-dimensional). Such a small $\Delta$ suggests the presence of the bare upper Hubbard band within the oxygen $p$ bandwidth and thus provides an example of a correlated covalent insulator. [S0163-1829(98)02103-1]

## I. INTRODUCTION

The one-dimensional cuprates and nickelates have attracted much attention in recent times due to the presence of interesting electronic and magnetic properties.[1–11] There have been extensive experimental investigations in such systems involving the transport and magnetic properties,[5–9] structural properties,[10,11] and the spin dynamics.[1–4] However, there have been few investigations using various techniques of high-energy spectroscopies. It is well known that such electron spectroscopic investigations, in conjunction with model many-body calculations, yield estimates of various electronic interaction strengths, such as the charge-transfer energy, Coulomb interaction strengths, and the hopping interaction strengths, thereby providing a quantitative description of the ground state in such strongly correlated electron systems. We have carried out detailed investigations of two closely related one-dimensional cuprates, $Ca_2CuO_3$ and $Sr_2CuO_3$, using various forms of electron spectroscopic techniques. From our studies we have estimated different interaction strengths and we discuss the similarities and differences in the electronic structures of these two compounds *vis a vis* cuprates with two- or three-dimensional crystal structures. Our results indicate interesting ground states in these compounds, particularly for $Sr_2CuO_3$ with a characteristically reduced charge-transfer energy.

The structure of $Sr_2CuO_3$ and $Ca_2CuO_3$, shown in Fig. 1(a), is $K_2NiF_4$-like (space group Immm) with the vacancy at the oxygen sites along the $a$ direction.[12] The lattice constants $a$, $b$, and $c$ are 3.48 Å, 3.91 Å, and 12.68 Å in $Sr_2CuO_3$ and 3.263 Å, 3.783 Å, and 12.262 Å in $Ca_2CuO_3$, respectively. The $CuO_4$ polyhedra are linked by sharing corners with the Cu-O-Cu angle to be 180° only along the $b$ direction. The $CuO_4$ units are perfect square in $Sr_2CuO_3$, but slightly distorted in $Ca_2CuO_3$ with a smaller Cu-O distance along the chain ($b$) direction.[10] The parallel Cu-O chains shifted along the $a$ direction in this structure do not couple significantly due to the absence of oxygen atoms in the edge center positions along the $a$ axis. The chains shifted along the $c$ axis also do not interact with each other due to the large separations involved. Thus, the electronic structure of these compounds is essentially governed by the one-dimensional Cu-O chains. Magnetic properties are also influenced by these structural aspects. The intrachain exchange interaction is very strong whereas the interchain interaction is very weak. The three-dimensional antiferromagnetic long-range order sets in only at a very low temperature ($T_N \approx 5$ K),[7] though

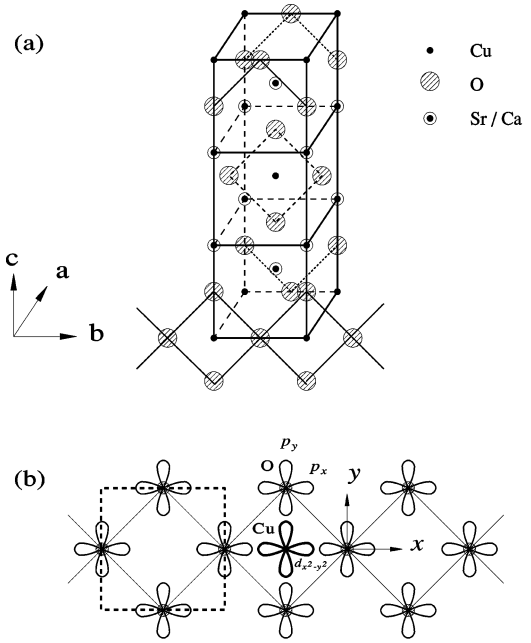


FIG. 1. (a) The crystal structure of $Sr_2CuO_3$ and $Ca_2CuO_3$ showing the one-dimensional character of the system. (b) The one-dimensional oxygen sublattice considered in the present problem obtained from the chain shown with the crystal structure. The relevant oxygen orbitals as well as the Cu $d_{x^2-y^2}$ orbital at the impurity site are also shown. The dotted line encloses the unit cell of the host oxygen 2$p$ lattice considered in the impurity calculation.

 

the value of the exchange interaction strength along the chain in $Sr_2CuO_3$ is unusually large [$\sim$0.26 eV (Ref. 7) or 0.19 eV (Ref. 8)] compared to that in other divalent compounds like $La_2CuO_4$ ($\sim$0.13 eV).[13] Thus, these compounds provide the prototypical examples of the one-dimensional spin-half systems. The transport measurements on these systems estimate an activation energy of about 0.18 eV in each case,[10] while the optical conductivity measurements suggest a considerably larger gap in $Ca_2CuO_3$ [$\sim$1.75 eV (Ref. 14)] and in $Sr_2CuO_3$ [$\sim$1.5 eV (Ref. 15)]. It has been reported[16] that the oxidized $Sr_2CuO_3$ shows superconductivity below 70 K.

In this work we study the electronic structure of $Sr_2CuO_3$ and $Ca_2CuO_3$ using various high-energy spectroscopic measurements. We calculate the valence-band and Cu $2p$ core-level spectra including all multiplet interactions to estimate different interaction strengths and to provide quantitative descriptions of the electronic structures in these two compounds.

## II. EXPERIMENT

$Sr_2CuO_3$ and $Ca_2CuO_3$ were prepared by solid-state reactions in air at 900° C for 24 h starting with stoichiometric amounts of $SrCO_3$, CuO, and $CaCO_3$, respectively. The obtained powders were further heated at 1000° C and 950° C for $Sr_2CuO_3$ and $Ca_2CuO_3$, respectively, with several grindings in between. The samples were characterized by x-ray powder diffraction (XRD) patterns obtained from a JEOL-8P x-ray diffractometer at room temperature. The XRD patterns show both of the samples to be single phasic. Electron spectroscopic measurements were carried out in a combined XPS-UPS-BIS spectrometer from VSW, after *in situ* scraping with an alumina file to obtain clean and reproducible surfaces at liquid-nitrogen temperature. The cleanliness was monitored by the impurity feature at the higher binding energy of the O 1*s* peak and the total C 1*s* signal. The resolution for the ultraviolet photoemission (UP) and x-ray photoemission (XP) spectroscopic measurements are 0.1 eV and 0.8 eV, respectively. In order to probe the unoccupied part of the electronic structure we have carried out the inverse photoemission spectroscopic measurements by varying the energy of the incident electrons from an electron gun and counting the photons at a fixed energy (1486.6 eV), known as bremsstrahlung isochromat spectroscopy (BIS) with a total resolution of 0.8 eV. In this case also the samples are scraped several times during the experiment to maintain a reproducible surface at liquid-nitrogen temperature.

## III. CALCULATIONAL DETAILS

Cluster calculations for the valence-band and core-level photoemission spectra were performed including all multiplet interactions within the $CuO_4$ cluster following our earlier work.[17] We include the full multiplet interactions within the Cu $d$ manifold with Racah parameters $B$ and $C$ fixed at 0.58 and 0.15 eV, respectively. The wave function of the ground state is given by a linear combination of $d^9$ and $d^{10}\underline{L}^1$ configurations, where $d$ and $\underline{L}$ denote the Cu 3$d$ electron and O $2p$ hole, respectively. The oxygen $2p$-to-Cu 3$d$ charge-transfer energy is defined by $\Delta = E(d^{10}\underline{L}^1) - E(d^9)$ and the 3$d$-3$d$ Coulomb interaction energy by $U_{dd} = E(d^{10}) + E(d^8) - 2E(d^9)$, where $E(d^n\underline{L}^m)$ is the center of gravity of the $d^n\underline{L}^m$ multiplets. The final states of the Cu 3$d$ photoemission are given by linear combinations of $d^8$, $d^9\underline{L}^1$ and $d^{10}\underline{L}^2$ configurations. The hybridization terms between Cu 3 $d$ and O $2p$ orbitals are expressed in terms of Slater-Koster parameters $(pd\sigma)$ and $(pd\pi)$. The ratio $(pd\sigma)/(pd\pi)$ is fixed at $-2.2$. For the Cu $2p$ core-level photoemission spectrum, the wave functions of the final states are given by linear combinations of $\underline{p}^1d^9$ and $\underline{p}^1d^{10}\underline{L}^1$ configurations, where $\underline{p}$ denotes Cu $2p$ core hole. The energy difference $E(\underline{p}^1d^{10}\underline{L}^1) - E(\underline{p}^1d^9)$ is given by $\Delta - U_{pd}$, where $U_{pd}$ is the multiplet-averaged Coulomb repulsion energy between the Cu $2p$ and Cu 3$d$ holes. Here, the ratio $U_{dd}/U_{pd}$ is fixed at 0.8 as before.[17] The multiplet coupling between the Cu $2p$ and Cu 3$d$ holes is included using Slater integrals $F^2$, $G^1$, and $G^3$, which are fixed to the free-ion values. The configuration dependence of the transfer integrals is taken into account in order to reproduce consistently the valence-band and core-level photoemission spectra using a single set of parameters. Here, the transfer integrals are multiplied by a reduction factor when a Cu 3$d$ or core hole is created. The reduction factor for the Cu 3$d$ hole creation is assumed to be 0.8 and that for the Cu $2p$ core hole creation to be 0.7.[18] The crystal-field splitting due to the nonorthogonality between the atomic O $2p$ and Cu 3$d$ orbitals has been taken into account.[17] The adjustable parameters within this model are thus, the charge-transfer energy $\Delta$, the multiplet averaged Coulomb interaction strength $U_{dd}$, the transfer integral $(pd\sigma)$, and the Coulomb interaction strength between the O $2p$ and Cu 3$d$ holes $V_{pd}$.

In order to include the effects of the finite oxygen $p$ bandwidth, we followed an earlier work[19,20] and carried out the core-level calculation within the Anderson impurity model with the Cu atom embedded in the oxygen sublattice with the real structure as shown in Fig. 1(b). Since Cu exists in the divalent $d^9$ configuration in the $D_{4h}$ symmetry, the single hole in Cu occupies only the $d_{x^2-y^2}$ orbital, while all other $d$ orbitals are fully filled and do not contribute to the electronic structure. Thus, we consider only the $d_{x^2-y^2}$ orbital at the Cu site along with the $p_x$ and $p_y$ orbitals at the oxygen sites as shown in the figure. We have considered only the one-dimensional lattice of the oxygen atoms, since the interchain interaction is weak in these systems. Thus, considering three oxygen atoms in the unit cell (each square in the figure, shown by dotted line) we obtain six oxygen $p$ bands including only the in-plane $2p_x$ and $2p_y$ orbitals in the tight-binding approximation; these are given by

$$\epsilon_k^{1,4} = \epsilon_p$$

$$\epsilon_k^{2,5} = \epsilon_p + \sqrt{2}\sqrt{(pp\sigma)^2 + (pp\pi)^2 - 2(pp\sigma)(pp\pi)\cos(k_x)}, \tag{1}$$

$$\epsilon_k^{3,6} = \epsilon_p - \sqrt{2}\sqrt{(pp\sigma)^2 + (pp\pi)^2 - 2(pp\sigma)(pp\pi)\cos(k_x)},$$

where $\epsilon_p$ is the bare $p$ level energy and, $(pp\sigma)$ and $(pp\pi)$ are usual Slater-Koster integrals.[21] The impurity Hamiltonian used for calculating the core-level spectra is given by

$$H=\sum_{ik\sigma}\epsilon_k^i n_{ik\sigma}+\sum_{\sigma}(\epsilon_d+U_{pd}n_c)n_{d\sigma}$$

$$+\sum_{ik\sigma}(V_{kd}^i a_{d\sigma}^\dagger a_{ik\sigma}+\text{H.c.})+U_{dd}n_{d\uparrow}n_{d\downarrow}, \qquad (2)$$

where $\epsilon_k^i$ are the oxygen $p$ band energies ($i=1$ to 6), $n_{ik\sigma}$ occupation number at $\epsilon_k^i$ with spin $\sigma$, $\epsilon_d$ is the $d$ hole energy, $U_{pd}$ is the repulsive interaction strength between a $d$ hole and a core hole, $n_c$ the number of core holes, $n_{d\sigma}$ is the occupation number of Cu $3d$ holes at energy $\epsilon_d$ with spin $\sigma$, $a_{d\sigma}^\dagger$ creates a $d$ hole with spin $\sigma$, and $a_{ik\sigma}$ annihilates a ligand hole in the ligand band with momentum $k$ and spin $\sigma$. $V_{kd}^i=\langle\psi^i(k,r)|H|d(r=0)\rangle$ is the hopping interaction strength between the oxygen $p$ band and Cu $d_{x^2-y^2}$ orbital, where $\psi^i(k,r)$ are the oxygen $p$ band eigenfunctions. $U_{dd}$ and $n_d$ are the on-site Coulomb interaction strength and the number of $d$ holes in the system. The charge-transfer energy, $\Delta\ [=E(d^{10}\underline{L}^1)-E(d^9)]$ is measured with respect to the middle of the oxygen $p$ band and is expressed as $(\epsilon_p-\epsilon_d)$.

However, instead of solving the problem in the momentum space with six bands ($i=1-6$), we perform the usual transformation:[22,23]

$$|V(\epsilon)|^2=\sum_{ik}|V_{kd}^i|^2\delta(\epsilon-\epsilon_k^i). \qquad (3)$$

Thus, the Hamiltonian can be rewritten as

$$H=\sum_{i\sigma}\epsilon_i n_{i\sigma}+\sum_{\sigma}(\epsilon_d+U_{pd}n_c)n_{d\sigma}$$

$$+\sum_{i\sigma}[V(\epsilon_i)a_{d\sigma}^\dagger a_{i\sigma}+\text{H.c.}]+U_{dd}n_{d\uparrow}n_{d\downarrow}. \qquad (4)$$

In Eq. (4) we have replaced the continuum band states by a set of $N$ discrete levels with energies $\epsilon_i$. This procedure with large $N(>6)$ is known[24] to provide results essentially identical with that obtained from $N=\infty$, when $V=\Sigma_i|V(\epsilon_i)|^2$ is kept constant. In the present calculation we have used $N=10$.

## IV. RESULTS AND DISCUSSION

We show the experimental valence band photoemission spectra of $Ca_2CuO_3$ excited with Mg $K\alpha$ (1253.6 eV) and He I (21.2 eV) radiations in Fig. 2. The two spectra are normalized at the most intense peak position. Here we find two distinct features as marked by the vertical lines. The spectral intensity is peaked around 3.5 eV binding energy for both of the photon energies; however, the relative intensity of the peak around 5 eV binding energy increases with the decrease in the incident photon energy. It is known[25] that the photoemission cross section for oxygen $p$ states dominates over Cu $d$ ones at lower energy of He I radiation; however, the relative cross section of oxygen $p$ rapidly decreases with the increasing photon energy leading to an increased contribution from Cu $d$ states with Mg $K\alpha$ photon source. Thus, the photoemission spectrum in the region between 4 and 6 eV binding energy arises primarily from the oxygen $2p$ like photoemission and 1–4 eV binding energy from the Cu $d$ states. This is indeed the usual behavior of other divalent cuprates in higher dimensions such as CuO (Ref. 26) and $La_2CuO_4$ (Ref. 27), which are examples of charge-transfer insulators.

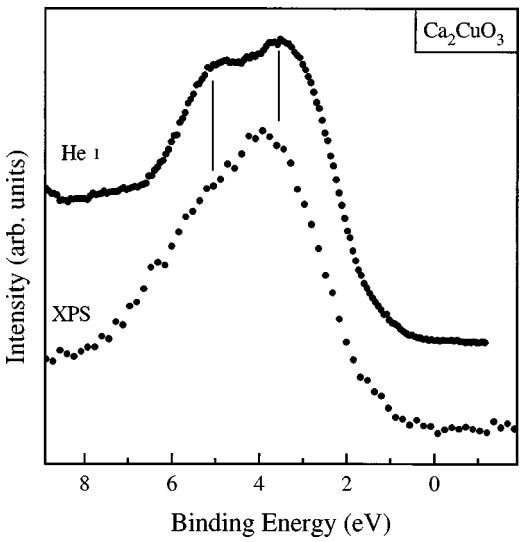


FIG. 2. The valence-band spectra of $Ca_2CuO_3$ with incident photon energies 1253.6 eV (XPS), and 21.2 eV (He I). The vertical lines indicate the positions of the two different features.

In Fig. 3 we show the valence-band spectra of $Sr_2CuO_3$ for the two photon energies. The most intense peak in the He I excited spectrum at about 3 eV binding energy decreases very rapidly relative to the other two features with increasing photon energy becoming the lowest-intensity feature in the x-ray excited spectrum. This suggests that this lowest-energy

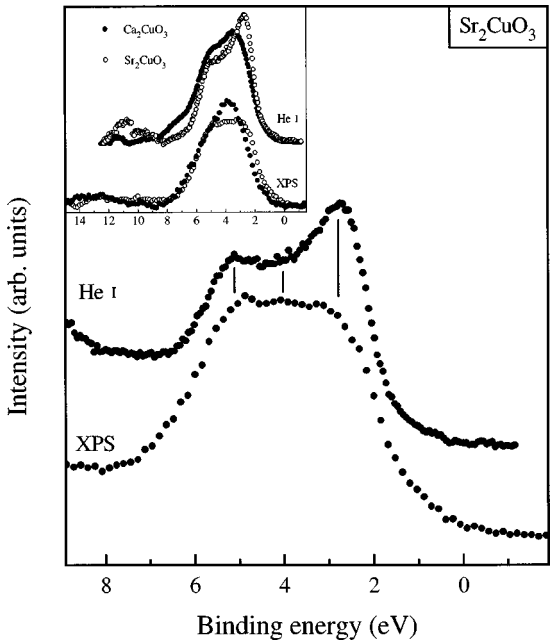


FIG. 3. The valence-band spectra of $Sr_2CuO_3$ with incident photon energies 1253.6 eV (XPS), and 21.2 eV (He I). The vertical lines indicate the positions of the three different features observed in the spectra. Inset shows the valence-band spectra of $Ca_2CuO_3$ (solid circles) and $Sr_2CuO_3$ (open circles) after normalizing to equal area under the curve and background subtraction.

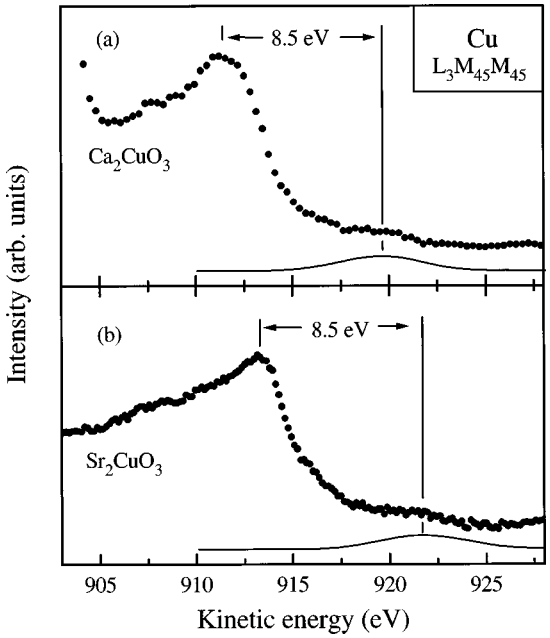


FIG. 4. (a) The Cu $L_3M_{45}M_{45}$ Auger spectrum of $Ca_2CuO_3$. The solid line shows the self-convoluted XP valence-band spectrum and coincides with the feature around 919.5 eV. Thus, the estimate of $U_{dd}$ in $Ca_2CuO_3$ is 8.5 eV, as shown in the figure. (b) Same as in (a), but for $Sr_2CuO_3$.

feature is primarily due to nonbonding oxygen $p$ states, while the Cu $d$ dominated spectral features at about 4–5 eV binding energy, are below the oxygen $p$ dominated energy region. This is a somewhat different situation compared to the known examples of the other divalent cuprates. For example, in the case of prototypical charge-transfer insulators like CuO (Ref. 26) [and also NiO (Ref. 28)], it was established by studying the spectral variations with photon energies, that the nonbonding oxygen $p$ emission appears at a higher binding energy with the leading peak in the spectra always being associated with transition-metal $d$ character. This is also the behavior in the case of $Ca_2CuO_3$ as illustrated in Fig. 2. The situation in Fig. 3 is reversed with the leading spectral feature having dominant nonbonding oxygen $p$ character, in sharp contrast to the classical examples of charge-transfer insulators. Besides the different photon energy dependence discussed above, the spectral features in $Sr_2CuO_3$ and $Ca_2CuO_3$ appear to be considerably different over a wide energy range, in spite of close structural similarities between the two compounds. We illustrate this by superposing the valence-band spectra of $Sr_2CuO_3$ and $Ca_2CuO_3$ in the inset of Fig. 3. Here we plot the spectra for both the photon energies by normalizing them with respect to the total area under the curve after background subtraction. It is clear from the figure that the spectral weight is shifted closer to the Fermi level in $Sr_2CuO_3$. The large enhancement in the spectral intensity of the near $E_F$ feature using the He I radiation in $Sr_2CuO_3$ proves that the leading edge of the electron removal spectrum in $Sr_2CuO_3$ is dominated by oxygen nonbonding states, in contrast to the other divalent Cu oxide systems including $Ca_2CuO_3$.

Figure 4(a) shows the Cu $L_3M_{45}M_{45}$ Auger spectrum corresponding to $Ca_2CuO_3$. There are two distinct features in the spectrum, one intense feature at about 911 eV and another weak one at 919.5 eV kinetic energies. In order to estimate $U_{dd}$, we compare the $L_3M_{45}M_{45}$ spectrum with the self-convoluted XP valence band spectrum representing the occupied part of the density of states. We plot the self-convoluted XP valence-band spectrum in the figure by solid line, which reproduces the weak feature obtained around 919.5 eV kinetic energy, establishing its origin from two uncorrelated holes in the final state of the Auger process. However, this self-convolution has no feature corresponding to the prominent feature around 911 eV. Thus, this spectral feature corresponds to a final state, where the two holes are on the same atomic site with intra-atomic Coulomb correlation strength between the two holes destabilizing the energy compared to the final state with two uncorrelated holes. Therefore, the energy difference between these two final states ($\sim$ 8.5 eV) provides an estimate of the on-site Coulomb correlation strength ($U_{1_G}$) for the most intense Auger peak ($^1G$) in this compound. We plot the corresponding Auger spectrum of $Sr_2CuO_3$ in Fig. 4(b). Here we find two distinct features around 913 eV and 921.5 eV in the spectrum. Once again the solid line representing the self-convoluted XP valence-band spectrum after the background subtraction compares well with the experimental feature around 921.5 eV. We find that the estimate of the on-site Coulomb correlation strength in $Sr_2CuO_3$ to be 8.5 eV, which is the same value as in the case of $Ca_2CuO_3$. Estimating various errors involved in determining the exact peak position, we obtain $8.5 \pm 0.3$ eV to be the Coulomb interaction strength in these compounds.

In order to obtain quantitative description of the electronic structures, we have analyzed *both* valence-band and core-level photoemission spectra of $Ca_2CuO_3$ and $Sr_2CuO_3$ using a consistent set of parameter strengths within configuration interaction model of a $D_{4h}$ $CuO_4$ cluster. We include the full multiplet interactions within the Cu $d$ manifold with the Racah parameters $B$ and $C$ fixed at 0.58 and 0.15 eV, respectively. The adjustable parameters within this model are the charge-transfer energy $\Delta$, the multiplet averaged on-site Coulomb interaction strength, $U_{dd}$, and the transfer integral expressed in terms of the Slater-Koster parameter $(pd\sigma)$ and the Coulomb interaction strength ($V_{pd}$) between the Cu $3d$ and O $2p$ orbitals. We have estimated the values of these parameters that best reproduce the valence-band photoemission spectra including the satellite structures observed. It was found that the valence band of $Ca_2CuO_3$ is best described by $U_{dd}=7.2$ eV, $(pd\sigma)=-1.5$ eV, $V_{pd}=0.8$ eV and $\Delta=0.5$ eV as shown in Fig. 5. It is to be noted here that the choice of multiplet interaction parameters $B$ and $C$ together with the multiplet averaged $U-$value suggests the effective $U_{1_G}$ for the most intense multiplet $^1G$ in the Auger spectrum to be 8.5 eV, in perfect agreement with the estimated value from the Auger spectra as discussed earlier. Interestingly, the valence-band spectrum of $Sr_2CuO_3$ can be simulated with all interaction strengths, such as $U_{dd}$, $V_{pd}$ and $(pd\sigma)$ the same as the case of $Ca_2CuO_3$, but with a reduced value of the charge-tansfer energy ($\Delta$) alone. The resulting best simulation with $\Delta=0.0$ eV is compared with the experimental spectrum of $Sr_2CuO_3$ in Fig. 5. While there is substantial amount of uncertainties ($\pm 0.5$ eV) in estimating a $\Delta$ value from the analysis of a single spectrum of a given compound, the

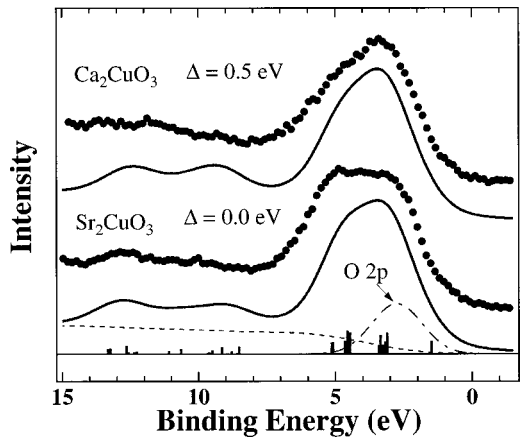


FIG. 5. Comparison between the experimental (dots) and calculated (solid lines) valence band spectra of $Ca_2CuO_3$ and $Sr_2CuO_3$. The dash-dotted lines shows the O $2p$ contribution. The dashed line is the background due to secondary electrons considered in both the cases.

present results suggest that the considerably different valence-band spectral features in these two otherwise closely related cuprates arise primarily from a reduction in the charge-transfer energy in $Sr_2CuO_3$. In order to ensure that this conclusion is also consistent with the core-level spectra, we have analyzed the Cu $2p$ spectra in these two compounds. The Slater integrals between the Cu $2p$ and $3d$ orbitals are $F^2=7.72$, $G^1=5.79$, and $G^3=3.29$ eV. In $Ca_2CuO_3$ the satellite structure related to the Cu $2p_{1/2}$ signal is strongly distorted by the Ca Auger line (Fig. 6), but the satellite structure accompanying the $2p_{3/2}$ signal allows a meaningful calculation of the core-level spectrum within the present model and, thus, extract parameter strengths. It is interesting to note that these core-level spectra can be well described with the same set of values of $U_{dd}$ (=7.2 eV), $V_{pd}$ (=0.8 eV), $(pd\sigma)$ (=−1.5 eV), and $\Delta$ (=0.5 eV in $Ca_2CuO_3$ and 0.0 eV in $Sr_2CuO_3$) as in the case of valence-band calculations (see Fig. 6). Since the energy difference between the main and satellite peaks is smaller in $Ca_2CuO_3$ than in $Sr_2CuO_3$, the spectrum of $Ca_2CuO_3$ is well reproduced by $\Delta$ larger than that of $Sr_2CuO_3$. Thus, the core-level spectra of these two compounds also suggest that the $\Delta$ value of $Sr_2CuO_3$ is somewhat smaller than that in $Ca_2CuO_3$. In order to compare the obtained interaction strengths from these one-dimensional cuprates to those obtained from other cuprates in a consistent way, we have analyzed Cu $2p$ XP spectra of CuO and $La_2CuO_4$ within the present model. These spectra can once again be reproduced by only adjusting $\Delta$, while keeping other parameter strengths fixed. The obtained $\Delta$'s are 1.5 eV for CuO and 1.0 eV for $La_2CuO_4$. Thus, there appears to be a systematic reduction in the value of $\Delta$ with the dimensionality of the crystal structure. It is known[29] that the charge-transfer energy is directly related to the Madelung potential of the system. Therefore, the decrease in Madelung potential with the dimensionality intrinsic to the crystal structure leads to a resulting reduction in the charge-transfer energy, suggesting the possibility of unusual electronic ground states in the low-dimensional systems.

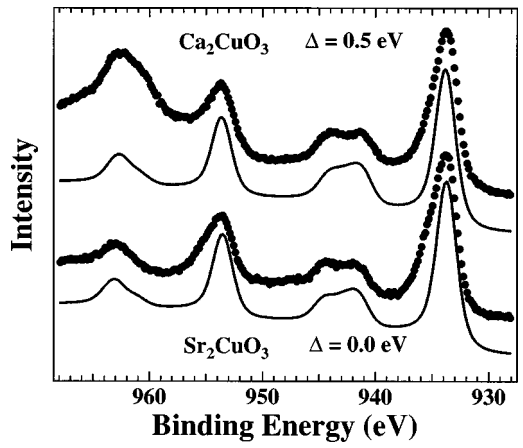


FIG. 6. Comparison between the experimental (dots) and calculated (solid lines) Cu $2p$ core-level spectra of $Ca_2CuO_3$ and $Sr_2CuO_3$.

It has been suggested[30] that the charge-transfer energy in $Sr_2CuO_3$ is as much as 2 eV lower than that in $La_2CuO_4$ based on multi-impurity cluster calculations. In their analysis, the charge-transfer energy for $Sr_2CuO_3$ was estimated to be 1.8 eV with the configuration dependence of the transfer integrals. The reason why their charge-transfer energy is by 1–2 eV larger than those obtained in the present study can be found in the definition of the charge-transfer energy. In their model, since only the $d_{x^2-y^2}$ orbital is considered, the charge-transfer energy is defined with respect to the $d_{x^2-y^2}$ orbital. On the other hand, in the present model, the charge-transfer energy is given by the energy difference between the O $2p$ orbital and the center of gravity of the $3d$ orbitals split by the crystal field, which is $\sim$ 1.0 eV smaller than that between the $d_{x^2-y^2}$ and O $2p$ orbitals.

In Fig. 7, we combine the UV photoelectron and bremsstrahlung isochromat (BI) spectra with a common Fermi energy in order to estimate the band gap. The BIS of $Ca_2CuO_3$ and $Sr_2CuO_3$ in the low-energy region are very similar. This region is contributed predominantly by Cu $d$ and oxygen $p$ states with negligible contribution from other states and exhibits a single peak feature at about 3.3 and 3 eV above Fermi energy, respectively. These features correspond to electronic transitions into the upper Hubbard band arising from the $d^9$ configuration of $Cu^{2+}$ state hybridized with the O $p$ states. The BIS results along with the UP spectra of these compounds shown in Fig. 7 are consistent with the interaction parameters deduced from the analysis of x-ray photoemission core-level and valence-band spectra earlier; this is demonstrated by the calculated bar diagrams shown in Fig. 7. While we can, in principle, estimate the intrinsic bandgaps in these materials from the combined UPS and BIS in the figure, a precise determination of the band edges is difficult from these experimental spectra, since these bands are significantly broadened by the resolution function associated with the experimental technique, particularly in the case of BI spectra. Thus, we adopt an approach that has been successfully used in the past in determining the band edges[31–33] and we obtain an estimate of the intrinsic band gap of about $1.7\pm0.3$ eV in $Ca_2CuO_3$ [see Fig. 7(a)]. This is similar to the value ($\sim$1.75 eV) obtained from the optical conductivity measurements reported earlier.[14] $Sr_2CuO_3$

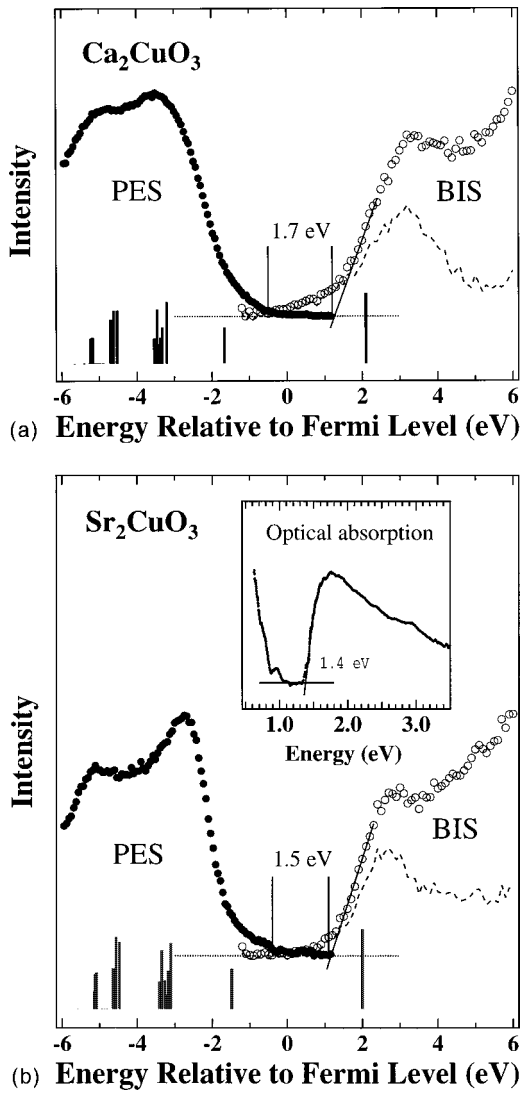


FIG. 7. (a) Combined UP and BI spectra of $Ca_2CuO_3$ suggesting a band gap of about 1.7 eV. The dashed line shows the BI spectrum after subtraction of linear background. (b) Combined UP and BI spectra of $Sr_2CuO_3$ suggesting a band gap of about 1.5 eV. The inset shows the optical absorption data showing the optical gap to be about 1.4 eV. The bar diagrams show the calculated valence-band and BI spectra in each case.

shows a band gap of about $1.5 \pm 0.3$ eV [see Fig. 7(b)]. This estimate is consistent with our optical absorption results (shown in the inset) as well as the results obtained in other groups.[15] This small reduction in the band gap ($\sim$ 0.2 eV) in $Sr_2CuO_3$ compared to $Ca_2CuO_3$ is related to the decrease of $\Delta$ in $Sr_2CuO_3$.

The above analysis of several spectroscopic data as well as of band gaps within a consistent set of interaction strengths clearly suggests that these one-dimensional cuprates are characterized by rather small values of the charge-transfer energy ($\Delta \sim 0.0$–$0.5$ eV). The bare oxygen $p$ bandwidth ($W$) is expected to be substantial ($\sim$ 2 eV) in these low-dimensional oxides. Noting that the charge-transfer energy $\Delta$, is measured with respect to the center of the oxygen $p$ band, these small values of $\Delta$ ($<W/2$) suggest that the bare upper Hubbard band lies within the oxygen $p$ derived band though they are insulators. However, it is to be realized that the neglect of the oxygen $p$ bandwidth implicit to the cluster model calculations leads to slightly renormalized smaller values of $\Delta$.[20,34] In order to ensure that our conclusion is not influenced by this limitation, we have calculated the Cu $2p$ core-level spectra of $Ca_2CuO_3$ and $Sr_2CuO_3$ within the Anderson impurity model including the effect of the oxygen $p$ bandwidth.[19] Considering both $p_x$ and $p_y$ orbitals on each oxygen atom in the one-dimensional lattice shown in Fig. 1 and an oxygen-oxygen interaction described in terms of Slater-Koster parametrization[21] [$(pp\sigma) = 0.4$ eV and $(pp\pi) = -0.2$ eV], we have calculated the hopping matrix element coupling the Cu $d_{x^2-y^2}$ orbital to the oxygen $p$ band as a function of energy over the bandwidth as described earlier.[19,34] The impurity calculation for the core-level spectrum including this dependence of the hopping matrix element on the energy and the oxygen $p$ bandwidth, gives $\Delta$ to be about 1.4 eV in the case of $Ca_2CuO_3$; this is larger ($\sim$0.9 eV) compared to the estimate from the previously discussed cluster approximation. When we apply the same impurity model to simulate the core-level spectrum of $Sr_2CuO_3$, we obtain a $\Delta$ value of about 0.8 eV with all the other parameter strengths same as obtained from the cluster calculation. As expected, this value is similarly larger than the estimation from the cluster calculation as in the case of $Ca_2CuO_3$. Such a small $\Delta$ value suggests that the bare upper Hubbard band is *within* the filled oxygen $p$ band, in conformity with the conclusions derived on the basis of cluster calculations.

According to the original classification in the Zaanen, Sawatzky, and Allen phase diagram,[35] such a material with the upper Hubbard band (UHB) within the $p$-bandwidth ($\Delta < W/2$) is expected to be metallic (barring band structure effects), in contrast to the insulating states of these compounds. In order to investigate if a Slater-type gap[36] ($U_{dd} = 0$) in contrast to the Mott-Hubbard gap ($U_{dd} > 0$), could open up in these compounds due to the antiferromagnetic order, we have performed *ab initio* spin-polarized band structure calculations within the local-spin-density approximation. This calculation is carried out using the linearized muffin-tin orbital method within the atomic sphere approximation. In the calculations, the convergence was obtained self-consistently taking $s$, $p$, and $d$ basis at each atomic sphere. The results obtained converging to the observed magnetic structure, show metallic ground states for both $Ca_2CuO_3$ and $Sr_2CuO_3$. Thus, it is clear that the band gap in this compound arises from strong electron-electron interactions and cannot be explained in terms of single particle effects, such as the doubling of the lattice periodicity due to the antiferromagnetic ordering. Some calculations[37,38] have however shown the possibility of an insulating ground state even when the UHB overlaps the oxygen $p$ band ($\Delta < W/2$) due to strong covalency effects; such an insulating state has been termed a correlated covalent insulator.[39] The main distinction between the idea of the correlated covalent insulator ($U > \Delta < W/2$) and that of the charge-transfer insulator ($U > \Delta > W/2$) is that the latter continues to be an insulator for any value of the hybridization interaction strength $t$, while the covalent insulating systems will transform into a metallic state with decreasing $t$ or covalency.[40] From these discussions and the estimated interaction strengths, it appears

that such one-dimensional cuprates most likely belong to or are very close to being in the correlated covalent insulating regime.

In conclusion, we have investigated the electronic structures of one dimensional cuprates $Ca_2CuO_3$ and $Sr_2CuO_3$ using various high-energy spectroscopies. We estimated different electron interaction strengths from analysis of the spectra in conjunction with model many-body calculations. It is found that the charge-transfer energy $\Delta$ is in general smaller in these compounds compared to other cuprates, such as $La_2CuO_4$ and CuO, though all other interaction parameters are similar. Such reduced values of $\Delta$ in one-dimensional cuprates suggest the possibility of an unusual electronic structure with the bare upper Hubbard band within the oxygen *p* bandwidth. This indicates that such low-dimensional systems can provide examples of correlated covalent insulators.

## ACKNOWLEDGMENTS

The authors thank Professor Y. Tokura for useful discussions and Professor C. N. R. Rao for continued support. The work in Bangalore was supported by the Department of Science and Technology, Government of India. The work in Tokyo was supported by a Grant-in-Aid for Scientific Research from the Ministry of Education, Culture, Sports and Science, Japan. K.M. thanks the Council of Scientific and Industrial Research, Government of India for financial assistance.

*Also at Jawaharlal Nehru Center for Advanced Scientific Research, Bangalore, India. Electronic address: sarma@sscu.iisc.ernet.in

[1] F.D.M. Haldane, Phys. Lett. **93A**, 464 (1983); Phys. Rev. Lett. **50**, 1153 (1983).
[2] I. Affleck, T. Kennedy, E.H. Lieb, and H. Tasaki, Phys. Rev. Lett. **59**, 799 (1987); P.P. Mitra, B.I. Halperin, and I. Affleck, Phys. Rev. B **45**, 5299 (1992).
[3] S. Ma, C. Broholm, D.H. Reich, B.J. Sternlieb, and R.W. Erwin, Phys. Rev. Lett. **69**, 3571 (1992).
[4] W.J.L. Buyers, R.M. Morra, R.L. Armstrong, M.J. Hogan, P. Gerlach, and K. Hirakawa, Phys. Rev. Lett. **56**, 371 (1986).
[5] E.S. Sörensen and I. Affleck, Phys. Rev. B **51**, 16 115 (1995).
[6] Y.J. Shin, E.D. Manova, J.M. Dance, P. Dordor, J.C. Grenier, E. Marquesteut, J.P. Doumere, M. Pouchard, and P. Hagenmuller, Z. Anorg. Allg. Chem. **616**, 201 (1992).
[7] H. Suzuura, H. Yasuhara, A. Furusaki, N. Nagaosa, and Y. Tokura, Phys. Rev. Lett. **76**, 2579 (1996).
[8] N. Motoyama, H. Eisaki, and S. Uchida, Phys. Rev. Lett. **76**, 3212 (1996).
[9] S. Kondoh, K. Fukuda, and M. Sato, Solid State Commun. **65**, 1163 (1988).
[10] D.R. Lines, M.T. Weller, D.B. Currie, and D.M. Ogbome, Mater. Res. Bull. **26**, 323 (1991).
[11] J.A. Alonso, I. Rasines, J. Rodriguez-Carvajal, and J.B. Torrance, J. Solid State Chem. **109**, 231 (1994).
[12] H. Müller-Buschbaum, Angew. Chemie **89**, 704 (1977).
[13] S. M. Hayden, G. Aeppli, R. Osborn, A.D. Taylor, T.G. Perring, S-W. Cheong, and Z. Fisk, Phys. Rev. Lett. **67**, 3622 (1991).
[14] Y. Tokura, S. Koshihara, T. Arima, H. Takaji, S. Ishibashi, T. Ido, and S. Uchida, Phys. Rev. B **41**, 11 657 (1990).
[15] Y. Tokura *et al.* (private communication).
[16] Z. Hiroi, Z. Takano, M. Asuma, and Y. Takeda, Nature (London) **364**, 315 (1993).
[17] T. Mizokawa, A. Fujimori, T. Arima, Y. Tokura, N. Mori, and J. Akimitsu, Phys. Rev. B **52**, 13 865 (1995).
[18] O. Gunnarsson and O. Jepsen, Phys. Rev. B **38**, 3568 (1988).
[19] D.D. Sarma and A. Taraphder, Phys. Rev. B **39**, 11 570 (1989).
[20] D.D. Sarma and S.G. Ovchinnikov, Phys. Rev. B **42**, 6817 (1990).
[21] J. C. Slater and G. F. Koster, Phys. Rev. **94**, 1498 (1954).
[22] O. Gunnarsson and K. Schönhammer, Z. Phys. B **30**, 297 (1978); Phys. Rev. B **28**, 4315 (1983).
[23] A. Bringer and H. Lustfeld, Z. Phys. B **28**, 213 (1977).
[24] A. Kotani, H. Mizuta, T. Jo, and J.C. Parlebas, Solid State Commun. **53**, 805 (1985).
[25] J.J. Yeh and I. Lindau, At. Data Nucl. Data Tables **32**, 1 (1985).
[26] J. Ghijsen, L.H. Tjeng, J. van Elp, H. Eskes, J. Westerink, G.A. Sawatzky, and M.T. Czyzyk, Phys. Rev. B **38**, 11 322 (1988).
[27] A. Fujimori, E. Takayama-Muromachi, Y. Uchida, and B. Okai, Phys. Rev. B **35**, 8814 (1987).
[28] G.A. Sawatzky and J.W. Allen, Phys. Rev. Lett. **53**, 2339 (1984).
[29] Y. Ohta, T. Tohyama, and S. Maekawa, Phys. Rev. Lett. **66**, 1228 (1991); Phys. Rev. B **43**, 2968 (1991).
[30] K. Okada, A. Kotani, K. Maiti, and D.D. Sarma, J. Phys. Soc. Jpn. **65**, 1844 (1996).
[31] A. Chainani, M. Mathew, D.D. Sarma, Phys. Rev. B **48**, 14 818 (1993); A. Chainani, Ph.D. thesis, I.I. Sc., Bangalore, India, 1992.
[32] A. Chainani, M. Mathew, and D.D. Sarma, Phys. Rev. B **47**, 15 397 (1993).
[33] K. Maiti and D.D. Sarma, Phys. Rev. B **54**, 7816 (1996).
[34] S. Nimkar, D.D. Sarma, and H.R. Krishnamurthy, Phys. Rev. B **47**, 10 927 (1993).
[35] J. Zaanen, G.A. Sawatzky, and J.W. Allen, Phys. Rev. Lett. **55**, 418 (1985).
[36] J.C. Slater, Phys. Rev. **82**, 538 (1951).
[37] D.D. Sarma, H.R. Krishnamurthy, S. Nimkar, S. Ramasesha, P.P. Mitra, and T.V. Ramakrishnan, Pramana **38**, L531 (1992).
[38] Seva Nimkar, D.D. Sarma, H.R. Krishnamurthy, and S. Ramasesha, Phys. Rev. B **48**, 7355 (1993).
[39] D.D. Sarma, J. Solid State Chem. **88**, 45 (1990).
[40] S.R. Barman, A. Chainani, and D.D. Sarma, Phys. Rev. B **49**, 8475 (1994).